Conformational Properties of 1-Fluoro-1-silacyclohexane, $C_5H_{10}SiHF$: Gas Electron Diffraction, Low-Temperature NMR, Temperature-Dependent Raman Spectroscopy, and Quantum Chemical Calculations†

Andras Bodi,‡ Ágúst Kvaran,‡ Sigridur Jonsdottir,‡ Egill Antonsson,‡ Sunna Ó. Wallevik,‡ Ingvar Arnason,*,‡ Alexander V. Belyakov,§ Alexander A. Baskakov,§ Margit Hölbling,⊥ and Heinz Oberhammer¶

Science Institute, University of Iceland, Dunhaga 3, IS-107 Reykjavik, Iceland, Saint-Petersburg State Technological Institute, Saint-Petersburg 190013, Russia, Institut für Anorganische Chemie, Technische Universität Graz, Stremayergasse 16, A-8010 Graz, Austria, and Institut für Physikalische and Theoretische Chemie, Universität Tübingen, 72076 Tübingen, Germany

Received August 21, 2007

The molecular structures of axial and equatorial conformers of 1-fluorosilacyclohexane, $C_5H_{10}SiHF$, as well as the thermodynamic equilibrium between these species were investigated by means of gas electron diffraction (GED), dynamic nuclear magnetic resonance, temperature-dependent Raman spectroscopy, and quantum chemical calculations (MP2, DFT, and composite methods). According to GED, the compound exists in the gas phase as a mixture of two conformers possessing the chair conformation of the six-membered ring and C_s symmetry and differing in the axial or equatorial position of the Si−F bond (axial = 63(8) mol %/equatorial = 37(8) mol %) at $T = 293$ K, corresponding to an A value of –0.31(20) kcal mol^{-1}. Density functional theory (DFT) calculations were employed to obtain the minimal energy path of the conformational inversion. The MP2, G3B3, and CBS-QB3 methods were also employed to calculate the equilibrium geometries and energies of the local minima in the gas phase and in solution. The gas-phase results are in good agreement with the experiment, whereas a combined PCM/IPCM(B3LYP/6-311G(d)) approach overestimates the stabilization of the axial conformer by 0.3−0.4 kcal mol^{-1} in solution at 112 K. Temperature-dependent Raman spectroscopy in the temperature ranges of 210–300 K (neat liquid), 120–300 K (pentane solution), and 200–293 K (dichloromethane solution) also indicates that the axial conformer is favored over the equatorial one by 0.25(5), 0.22(5), and 0.28(5) kcal mol^{-1} (ΔH values), respectively.

Introduction

The conformational behavior of six-membered ring systems, steric effects of substituents, and stereoelectronic interactions in the ring systems continue to be an active field of research.[2–8] Cyclohexane and its derivatives play an important role in organic stereochemistry. The Gibbs free energy difference between axial and equatorial conformations in monosubstituted cyclohexanes has been used as a measure of the inherent conformational properties of the substituent. With the rare exception o

Scheme 1

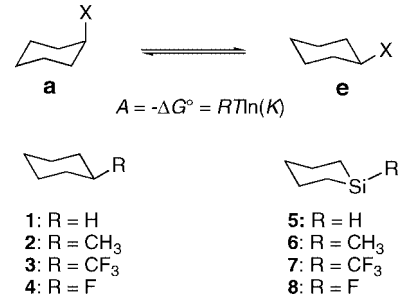

f substituents having mercury bonded to the cyclohexane ring, a general preference for the equatorial conformer is found.[9] Consequently, a positive A value (see Scheme 1 for the definition of A) corresponds to a preference for the equatorial conformer. The equatorial preference of methyl, ethyl, and isopropyl groups as substituents in cyclohexane has been reinvestigated in 1999. The A value of the methyl group was found to be 1.80(2) kcal mol^{-1} by low-temperature ^{13}C NMR spectroscopy and 1.98 kcal mol^{-1} by high-level ab initio calculations.[10] Compared with

* To whom correspondence should be addressed. E-mail: ingvara@raunvis.hi.is.

† Conformations of Silicon-Containing Rings. 7. For Part 6, see ref 1.

‡ University of Iceland.
§ Saint-Petersburg State Technological Institute.
⊥ Technische Universität Graz.
¶ Universität Tübingen.

(1) Girichev, G. V.; Giricheva, N. I.; Bodi, A.; Gudnason, P. I.; Jonsdottir, S.; Kvaran, A.; Arnason, I.; Oberhammer, H. *Chem. Eur. J.* **2007**, *13*, 1776.
(2) Alabugin, I. V. *J. Org. Chem.* **2000**, *65*, 3910.
(3) Alabugin, I. V.; Zeidan, T. A. *J. Am. Chem. Soc.* **2002**, *124*, 3175.
(4) Cuevas, G.; Juaristi, E. *J. Am. Chem. Soc.* **2002**, *124*, 13088.
(5) Leventis, N.; Hanna, S. B.; Sotiriou-Leventis, C. *J. Chem. Educ.* **1997**, *74*, 813.
(6) Ribeiro, D. S.; Rittner, R. *J. Org. Chem.* **2003**, *68*, 6780.
(7) Taddei, F.; Kleinpeter, E. *J. Mol. Struct. (Theochem)* **2004**, *683*, 29.
(8) Taddei, F.; Kleinpeter, E. *J. Mol. Struct. (Theochem)* **2005**, *718*, 141.
(9) Bushweller, C. H. In *Conformational Behavior of Six-Membered Rings* Juaristi, E., Ed.; VCH Publishers, Inc.: New York, 1995; p 25.
(10) Wiberg, K. B.; Hammer, J. D.; Castejon, H.; Bailey, W. F.; DeLeon, E. L.; Jarret, R. M. *J. Org. Chem.* **1999**, *64*, 2085.

10.1021/om7008414 CCC: $37.00
Publication on Web 11/27/2007

cyclohexane (**1**), much less is known about silacyclohexane (**5**) and its derivatives. The molecular structure of **5** has been determined by gas electron diffraction (GED)[11] and microwave spectroscopy (MW).[12] A theoretical study on the potential energy surface of **5** has been reported,[13] and the path for its chair-to-chair interconversion has been calculated.[13,14] Reports on monosubstituted silacyclohexanes are rather limited; however, interesting results have emerged so far. Controversial *A* values have been published for 1-methyl-1-silacyclohexane (**6**). The *A* value of **6** had first been reported to be negative based on investigations of ^{1}H NMR measurements at room temperature[15] and force field calculations.[16,17] In a more recent investigation, we were able to show from GED, low-temperature NMR, and quantum chemical (QC) calculations that *A* for the methyl compound **6** truly is positive, albeit its value is much lower than that for **2**.[18] The microwave spectrum of **6** revealed that **6e** and **6a** are similarly stable at room temperature.[19] Substitution of the methyl group in **2** with a trifluorometyl group causes the *A* value to increase to 2.5 kcal mol^{-1} in **3**.[20] Recently, we have also investigated the effect of substituting the methyl group in **6** for a trifluoromethyl group in **7**. According to a GED experiment at 293 K, the *A* value is −0.19(29) kcal mol^{-1} for the gas phase, whereas ^{19}F NMR measurements performed at 113 K gave a substantially higher *A* value of 0.4(1) kcal mol^{-1} for the solvent phase. These seemingly contradictory experimental findings were remarkably well reproduced by QC calculations.[1]

The conformational properties of methyl- and trifluoromethyl-substituted silacyclohexanes are, thus, in contrast with those of the corresponding cyclohexane derivatives. The reported Gibbs free energy differences for monosubstituted halo derivatives of cyclohexane show that the equatorial conformer is favored over the axial one by about 0.3 kcal mol^{-1} for fluorocyclohexane **4** and by about 0.5–0.7 kcal mol^{-1} for the chloro-, bromo-, and iodocyclohexane.[9,21–26] The axial conformer of the title compound, 1-fluoro-1-silacyclohexane (**8**), has been found to be lower in energy than the equatorial one by 0.12(7) kcal mol^{-1} based on the room temperature microwave spectrum.[27] In the present paper, we further investigate this compound and report its conformational analysis using GED, low-temperature ^{19}F NMR, temperature-dependent Raman spectroscopy, and QC calculations.

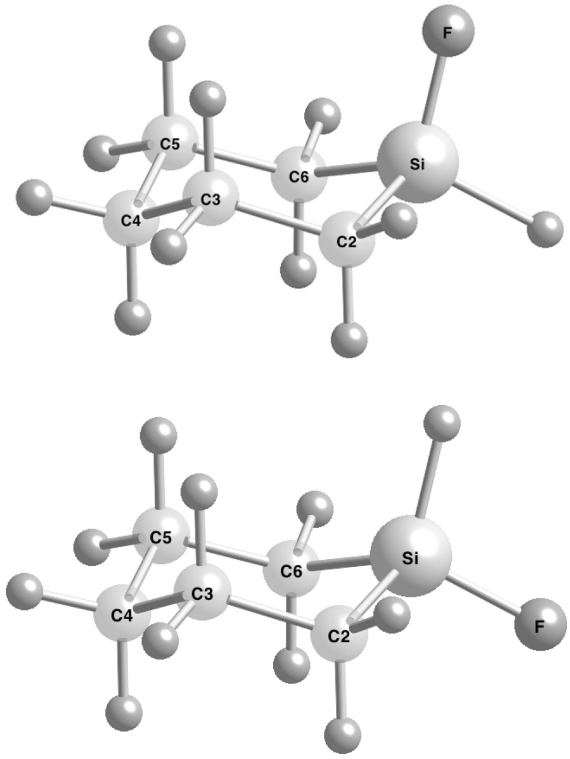

Figure 1. Structural models of axial **8a** (above) and equatorial **8e** (below) conformers for **8** with atom numbering.

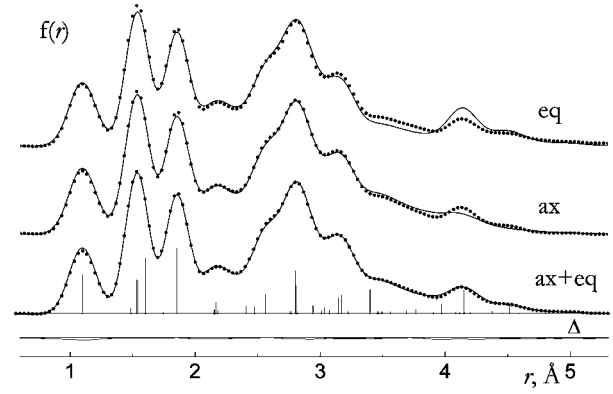

Figure 2. Radial distribution functions for geometries of the axial and equatorial conformers of **8** as well as for the mixture (experimental, dots; calculated, full line). At the bottom is the difference curve for the mixture.

Results and Discussion

GED Analysis. Structure refinements were carried out with least-squares analysis of the experimental molecular intensity curve. According to QC calculations, two stable conformers of $C_5H_{10}SiHF$ exist (Figure 1): the axial, **8a**, and the equatorial, **8e**. Each form possesses C_s symmetry with chair conformation of the six-membered ring.

Figure 2 compares observed and calculated radial distribution curves separately for axial and equatorial conformers. The two calculated curves differ substantially in the region $r > 3$ Å, which corresponds predominantly to nonbonded distances between the fluorine and ring atoms. This demonstrates that the electron diffraction intensities are sensitive toward the conformational properties of this compound. Comparison with the experimental radial distribution function, which was derived by Fourier transformation of the molecular intensities, confirms that

(11) Shen, Q.; Hilderbrandt, R. L.; Mastryukov, V. S. *J. Mol. Struct.* **1979**, *54*, 121.
(12) Favero, L. B.; Caminati, W.; Arnason, I.; Kvaran, A. *J. Mol. Spectrosc.* **2005**, *229*, 188.
(13) Arnason, I.; Thorarinsson, G. K.; Matern, E. *Z. Anorg. Allg. Chem.* **2000**, *626*, 853.
(14) Arnason, I.; Kvaran, Á.; Bodi, A. *Int. J. Quantum Chem.* **2006**, *106*, 1975.
(15) Carleer, R.; Anteunis, M. J. O. *Org. Magn. Reson.* **1979**, *12*, 673.
(16) Frierson, M. R.; Iman, M. R.; Zalkow, V. B.; Allinger, N. L. *J. Org. Chem.* **1988**, *53*, 5248.
(17) Ouellette, R. J. *J. Am. Chem. Soc.* **1974**, *96*, 2421.
(18) Arnason, I.; Kvaran, A.; Jonsdottir, S.; Gudnason, P. I.; Oberhammer, H. *J. Org. Chem.* **2002**, *67*, 3827.
(19) Favero, L. B.; Velino, B.; Caminati, W.; Arnason, I.; Kvaran, A. *Organometallics* **2006**, *25*, 3813.
(20) Della, E. W. *J. Am. Chem. Soc.* **1967**, *89*, 5221.
(21) Caminati, W.; Damiani, D.; Scappini, F. *J. Mol. Spectrosc.* **1984**, *104*, 183.
(22) Caminati, W.; Scappini, F.; Damiani, D. *J. Mol. Spectrosc.* **1984**, *108*, 287.
(23) Damiani, D.; Ferretti, L. *Chem. Phys. Lett.* **1973**, *21*, 592.
(24) Pierce, L.; Beecher, J. F. *J. Am. Chem. Soc.* **1966**, *88*, 5406.
(25) Pierce, L.; Nelson, R. *J. Am. Chem. Soc.* **1966**, *88*, 216.
(26) Scharpen, L. H. *J. Am. Chem. Soc.* **1972**, *94*, 3737.
(27) Favero, L. B.; Velino, B.; Caminati, W.; Arnason, I.; Kvaran, A. *J. Phys. Chem. A* **2006**, *110*, 9995.

both conformers are present in the vapor under the conditions of the electron diffraction experiment, with the axial form being more abundant.

Least-squares refinement of the structural parameters was performed with the use of a modified version of the *KCED25 M* computer program.[28,29] Scattering amplitudes and phases of ref 30 were used. The geometry of the six-membered ring was described by three bond lengths (Si−C2, C2−C3, and C3−C4), two bond angles (C2−Si−C6 and C3−C4−C5), and the two flap angles between the C2SiC6 (flap(Si)) or C3C4C5 (flap(C4)) plane and the C2C3C5C6 plane. The orientation of the Si−F and C4−H_{ax} bonds was described by two dummies X1 and X2, situated on the bisector of the adjacent endocyclic angles C2−Si−C6 and C3−C4−C5, respectively. To reduce the number of refined parameters, the following assumptions were made on the basis of the MP2 results. Only the geometric parameters of the prevailing axial conformer were refined, and the parameters of the equatorial form were tied to those of the axial conformer using the calculated differences. For the axial conformer, the difference between the nearly equal C2−C3 and C3−C4 bond lengths was constrained to the calculated value. The C−H bonds and H−C−H angles were described by one internal coordinate for each set, and all H_{ax}−C2−C3, H_{eq}−C3−C2, H_{eq}−C3−C4, and H_{ax}−C3−C2 angles were set equal. Angles that define the orientation of the C−H bonds were set to calculated values. Theoretical values for geometrical parameters and vibrational amplitudes were used as initial approximations. Cartesian coordinates of the atoms were calculated in terms of a geometrically consistent r_{h1} structure. Mean amplitudes and shrinkage corrections, $r_{h1} - r_a$, were calculated from MP2 force constants with the *SHRINK* program, which takes nonlinear transformation of internal and Cartesian coordinates into account.[31,32] The vibrational amplitudes were divided into two groups in the least-squares refinement, one for bonded distances and the other for nonbonded distances. In each group, amplitudes were refined with the fixed differences from MP2 calculations. With the above assumptions, 10 structural parameters (see Table 1), two groups of vibrational amplitudes, the mole fraction of the axial conformer, and two scale factors were refined simultaneously. Because this refinement resulted in a very good agreement between experimental and calculated intensities, we decided not to increase the number of parameters by refining additional groups of vibrational amplitudes. The final values of the refined parameters are presented in Tables 1 and 2. Three correlation coefficients had absolute values larger than 0.7: Si−F/C2−C3 = −0.77; flap(Si)/C2−Si−C6 = −0.74; flap(Si)/F−Si−X1 = 0.78. All interatomic distances, vibrational amplitudes, and Cartesian coordinates and the radial distribution curve are given in the Supporting Information.

Table 1 compares geometrical parameters derived by GED, QC methods, and MW. Both QC methods, B3LYP and MP2, overestimate Si−C and Si−F bond lengths. All other geometrical parameters are in good agreement with the experimental values within their experimental uncertainties. The GED and MW results also agree with each other within their respective uncertainties.

Table 1. Experimental and Calculated Geometric Parameters of the Axial Conformer of $C_5H_{10}SiHF$ (in Å and deg; C_s Symmetry)[a]

	GED (r_a, ∠$_{h1}$) structure	B3LYP/ 6-31G(d,p) r_e structure	MP2/6-(31G (d,p) r_e structure	MW[b] r_0 structure
Si−C p_1[c]	1.854(2)	1.877	1.869	1.866(12)
Si−F_{ax} p_2	1.605(5)	1.627	1.631	1.620(21)
Si−F_{eq} (p_2)	1.602(5)	1.624	1.628	1.624(21)
C2−C3 p_3	1.541(5)	1.547	1.539	1.537(21)
C3−C4 (p_3)	1.532(5)	1.540	1.532	1.526(18)
$(C-H)_{mean}$ p_4	1.099(3)	1.098	1.093	
Si−H	1.487[d]	1.490	1.478	
F−Si−H	106.5[d]	106.4	106.7	
C2−Si−C6 p_5	105.2(7)	105.9	105.4	106.1(9)
C3−C4−C5 p_6	113.6(17)	114.5	114.2	114.3(12)
F−Si−$X1_{ax}$ p_7	121.8(42)[e]	123.9	122.7	121.4(12)
F−Si−$X1_{eq}$ p_8	126.8(25)	126.4	126.9	126.4(6)
$(H-C-H)_{mean}$	106.4[d]	106.0	106.4	
$flap(Si)_{ax}$ p_9	40.0(41)	38.0	41.4	39.8(12)
$flap(Si)_{eq}$ (p_9)	42.8(41)	41.7	44.2	43.8(6)
flap(C4) p_{10}	57.8(10)	56.8	57.9	58.0(15)
H_{ax}−C4−X2	127.3[d,e]	127.6	127.3	
H_{eq}−C2−Si	112.0[d]	111.3	111.7	
H_{eq}−C2−C3	110.6[d]	110.7	110.6	
H_{ax}−C2−C3	109.4[d,f]	109.5	109.2	

[a] Atom numbering is given in Figure 1. Error limits are $3\sigma_{LS}$ values. [b] Reference 27. [c] p_i = refined parameter; (p_i) = the difference with parameter p_i set to the MP2 calculated value; unless specified, the observed parameter is the average for the two conformers. [d] Not refined. [e] Xi = dummy atom on the bisector of the adjacent endocyclic angle. [f] H_{ax}−C2−C3 = H_{eq}−C3−C2 = H_{eq}−C3−C4 = H_{ax}−C3−C2.

Table 2. Interatomic Distances, Experimental and Calculated Vibrational Amplitudes, and Vibrational Corrections (without Nonbonded Distances Involving H Atoms) for the Axial Conformer 8a (in Å)[a]

	r_a	l_{exp}	l_{calc}[c]	$\Delta r = r_{h1} - r_a$	group[d]
C−H	1.099(3)	0.080(2)[b]	0.076	0.0015	1
C2−C3	1.541(5)	0.055(2)	0.051	0.0006	1
C3−C4	1.532(5)	0.054(2)	0.050	0.0003	1
Si−H	1.487_{fixed}	0.090(2)	0.087	0.0014	1
Si−C2	1.854(2)	0.055(2)	0.051	0.0006	1
Si−F	1.605(5)	0.046(2)	0.042	0.0002	1
C2···C4	2.561(14)	0.075(3)	0.070	0.0046	2
C3···C5	2.561(25)	0.074(3)	0.069	0.0045	2
Si···C3	2.802(24)	0.084(3)	0.079	0.0069	2
C2···C6	2.942(15)	0.087(3)	0.083	0.0053	2
C2···F	2.808(40)	0.098(3)	0.093	0.0060	2
C2···C5	3.145(14)	0.087(3)	0.083	0.0077	2
Si···C4	3.171(16)	0.081(3)	0.077	0.0092	2
C3···F	3.399(46)	0.199(3)	0.194	0.0176	2
C4···F	3.973(64)	0.188(3)	0.184	0.0210	2

[a] For atom numbering, see Figure 1. [b] Error limits are $3\sigma_{LS}$ values. [c] MP2/6-31G(d,p). [d] Group of refined amplitudes.

The Si−C2 bond distance depends strongly on the electronegativity of the substituent X (X = H, CH_3, CF_3, and F) in substituted silacyclohexanes. The bond length shortens with increasing electronegativity,[33,34] χ, from 1.885(3) Å[11] for X = H (χ = 2.08) to 1.867(4) Å[18] for X = CH_3 (χ = 2.17), to 1.856(3) Å[1] for X = CF_3 (χ = 3.46), and to 1.854(2) Å for X = F (χ = 4.00). This trend mirrors the one observed for 1,1-disubstituted silacyclobutanes.[35] The shortening of the Si−C2 bond with increasing electronegativity of X can be rationalized in terms of two effects, the reduced covalent radius of silicon

(28) Andersen, B.; Seip, H. M.; Strand, T. G.; Stolevik, R. *Acta Chem. Scand.* **1969**, *23*, 3224.
(29) Gundersen, G.; Samdal, S.; Seip, H. M. *Least Squares Structural Refinement Program Based on Gas Electron-diffraction Data*; Department of Chemistry, University of Oslo: Oslo, Norway, 1981; Vols. *I−III*, p 116.
(30) Ross, A. W.; Fink, M.; Hilderbrandt, R. L. *International Tables of Crystallography*; Kluwer, C., Ed.; Academic Publishers: Dordrecht, The Netherlands, 1992; p 245.
(31) Sipachev, V. A. *J. Mol. Struct. (Theochem)* **1985**, *121*, 143.
(32) Sipachev, V. A. *Vibrational effects in diffraction and microwave experiments: A start on the problem*; JAI Press: New York, 1999; Vol. 5, p 263.
(33) Hati, S.; Datta, D. *J. Comput. Chem.* **1984**, *13*, 912.
(34) Mullay, J. *J. Am. Chem. Soc.* **1985**, *107*, 7271.
(35) Novikov, V. P.; Tarasenko, S. A.; Samdal, S.; Shen, Q.; Vilkov, L. V. *J. Mol. Struct.* **1999**, *477*, 71.

Table 3. Conformational Properties of 8

T (K)	method/basis set	$\Delta E = E_{ax} - E_{eq}$ (kcal mol^{-1})	$\Delta H = H_{ax} - H_{eq}$ (kcal mol^{-1})	$A = G_{ax} - G_{eq}$ (kcal mol^{-1})	mol % axial
298	B3LYP/6-31G(d,p)	−0.23		−0.27	61
298	MP2/6-31G(d,p)	−0.12		−0.15	56
298	CBS-QB3	−0.18		−0.18	57
298	G3B3	−0.16		−0.16	56
298	MW[a]	−0.12(7)			
293	GED			−0.31(20)	63(8)
300–210	Raman, neat		−0.25(5)[b]		
300–120	Raman, in pentane		−0.22(5)[b]		
293–200	Raman, in CH_2Cl_2		−0.28(5)[b]		
112	G3B3/PCM[c]	−0.43		−0.45	88
112	G3B3/PCM[d]	−0.52		−0.54	92
112	NMR[e]			−0.13(2)	64(2)

[a] Reference 27. [b] Average value from van't Hoff plots using peak areas and heights. [c,d] G3B3 0 K electronic energies with ZPE and thermal contributions in solution calculated in CH_2Cl_2 (*c*) and $CHCl_3$ (*d*) solution with the PCM method; the solvent effects on the electronic energy are taken into account with the IPCM method (see text). [e] Measured in a 1:1:3 mixture of CD_2Cl_2, $CHFCl_2$, and CHF_2Cl.

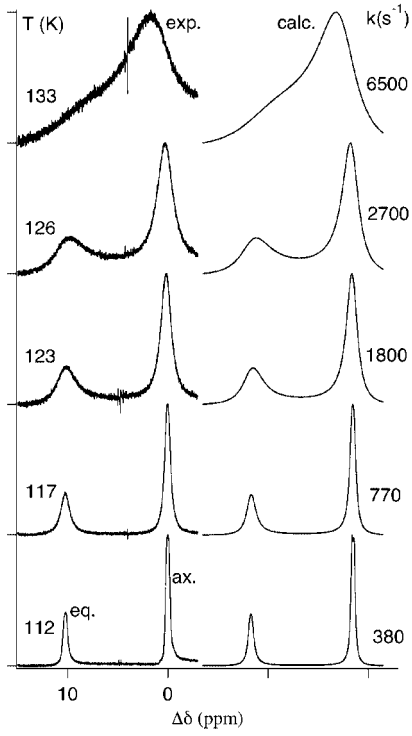

Figure 3. Simulation of ^{19}F NMR spectra for **8** in a 1:1:3 mixture of CD_2Cl_2, $CHFCl_2$, and CHF_2Cl. Experimental spectra are on the left and calculated on the right.

and the increased polar contribution of the $Si^{+}-C^{-}$ bond. The other geometric parameters of the silacyclohexane ring do not change more than their experimental uncertainties in the X = H, CH_3, CF_3, and F substituted silacyclohexane series.

According to the GED data, the axial conformer **8a** has a 63(8) mol % abundance in the vapor of **8** at 293 K. This value corresponds to an A value of −0.31(20) kcal mol^{-1} (Table 3).

NMR Spectroscopy. The ^{19}F NMR spectra at room temperature and down to about 135 K show rapid interconversion of **8e** and **8a**. On cooling below 135 K, the spectrum (Figure 3) shows line broadening and a gradual splitting of the Si−F signal into two components with the larger one at lower frequency, indicating a mixture of two conformers. As a general rule in cyclohexane chemistry, the resonance signal of a substituent in the axial position has a lower δ value than the signal for the same substituent in the equatorial position.[36–38] Therefore, the larger signal may be assigned to the axial conformer **8a**. This assignment is further supported by calculated ^{19}F chemical shifts for **8e** and **8a** (see below). Dynamic NMR (DNMR) simulations of the spectra allowed the determination of the rate constants and equilibrium constants (hence free-energy changes) for the conformational inversion of **8** as well as the corresponding free energies of activation as a function of the temperature. The derived rate constants indicate slightly increasing $\Delta G^{\#}$ values with temperature in the 109−133 K range, as shown in Figure 4. Thus, at 112 K, $\Delta G^{\#}_{e\to a} = 5.0$ kcal mol^{-1}, $K_{e\to a} = 1.79$, and $\Delta G_{e\to a} = -0.13(2)$ kcal mol^{-1} have been found.

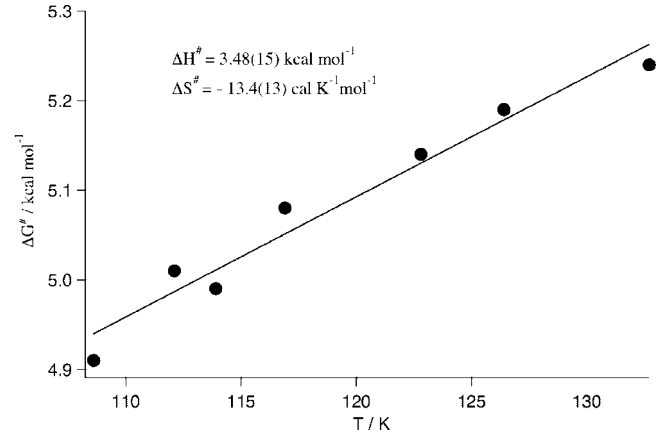

Figure 4. Gibbs free energies of activation ($\Delta G^{\#}$) for equatorial to axial conformational inversion of **8**. Corresponding average $\Delta H^{\#}$ and $\Delta S^{\#}$ values for the temperature range (110–130 K) are derived from the expression $\Delta G^{\#} = \Delta H^{\#} - T\Delta S^{\#}$.

Raman Spectroscopy. The van't Hoff relation $\ln(A_a/A_e) = -\Delta H_{e\to a}/RT +$ constant was used to analyze temperature-dependent Raman spectra of **8**. A_a and A_e are the line intensities (either peak heights or areas) originating from the axial and equatorial conformers of **8**. The Raman scattering coefficients for conformers **8a** and **8e** were assumed to be independent of the temperature in the data analysis.[39]

The Raman spectrum of the pure compound is shown in Figure 5. The two bands at 630 and 658 cm^{-1} were assigned to the symmetric Si−C stretching modes (A') in **8a** and **8e**,

(36) Aliev, A. E.; Harris, K. D. M. *J. Am. Chem. Soc.* **1993**, *115*, 6369.
(37) Booth, H. In *Progress in NMR Spectroscopy*; Pergamon Press: Oxford, U.K., 1969; Vol. 5, p 149.
(38) Kalinowski, H.-O.; Berger, S.; Braun, S. *^{13}C NMR Spektroskopie*; Georg Thieme Verlag: Stuttgart, Germany, 1984.
(39) Klaeboe, P. *Vib. Spectrosc.* **1995**, *9*, 3.

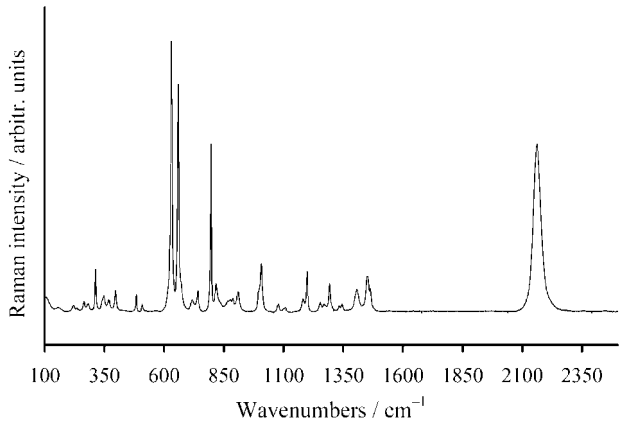

Figure 5. Raman spectrum of pure compound **8** at room temperature.

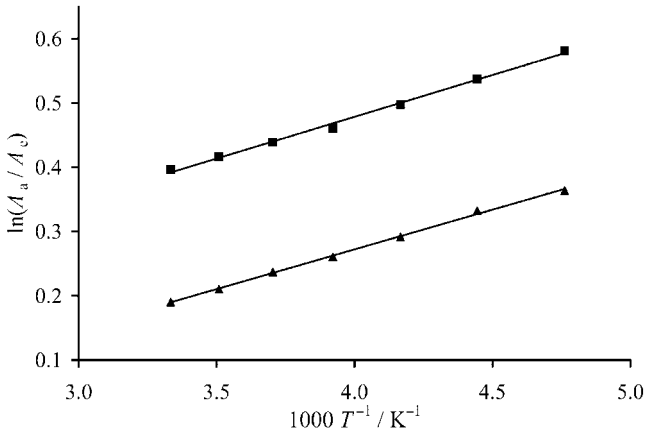

Figure 6. van't Hoff plot of the band pair 630/658 cm^{-1} of pure **8** using peak areas (above) and peak heights (below).

respectively, based on B3LYP/6-31G(d,p) calculations (the calculated frequencies are 620 and 652 cm^{-1}, respectively). The fit enthalpies of conformational inversion based on the van't Hoff plot of the band pair 630/658 cm^{-1} of pure **8** are $\Delta H_{e\rightarrow a} = -0.26$ kcal mol^{-1} (peak areas) and -0.25 kcal mol^{-1} (peak heights) (Figure 6). Similarly, temperature-dependent Raman spectra of **8** were also recorded in a pentane solution and in dichloromethane. Peak areas and heights were analyzed separately in each case. The average $\Delta H_{e\rightarrow a}$ values from peak areas and heights are presented in Table 3. Tabulated peak positions and intensities in the Raman spectrum are available as Supporting Information. The different polarity of the medium does not influence the ΔH values, and they remain constant in the neat liquid and in pentane and dichloromethane solutions within their experimental uncertainties.

Computational Studies in the Gas Phase. The minimum-energy path for the chair-to-chair inversion of **8** has been calculated in redundant internal coordinates with the STQN-(Path) method as implemented in *Gaussian 03*[40] at the B3LYP/6-311+G(d,p) level of theory. Similarly to the trifluoromethyl derivative **7**,[1] the path was obtained in four slices using the keyword OPT(QST3,PATH=11), i.e., from minimum **8a** to **8b**, from **8b** to **8c**, from **8c** to **8d**, and from **8d** to **8e**, as shown in Figure 7. The inversion path from the axial conformer, **8a**, consists of a half-chair/sofalike transition state from which the molecule can move into a twist form of relatively high energy,

(40) Frisch, M. J.; Trucks, G. W.; Schlegel, H. B., *Gaussian 03*, revision C.02; Gaussian, Inc.: Wallingford. CT, 2004.

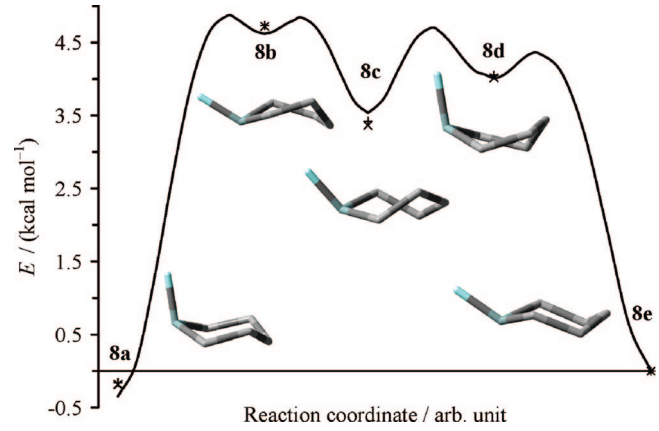

Figure 7. B3LYP/6-311+G(d,p) minimum-energy path for the chair-to-chair inversion of **8**. CBS-QB3 and G3B3 ZPE-corrected 0 K relative energies are plotted as crosses and pluses, respectively.

Table 4. Relative 0 K Energies, 298 K Free Energies, and Partial Abundances of 8a−e in the Gas Phase

	$\Delta E_{0\,K}$ (kcal mol^{-1})		$\Delta G_{298\,K}$ (kcal mol^{-1})		partial abundance (%)	
	CBS-QB3	G3B3	CBS-QB3	G3B3	CBS-QB3	G3B3
8a	−0.18	−0.16	−0.18	−0.16	57	56
8b	4.72	4.73	4.30	4.32	0.03	0.03
8c	3.36	3.42	3.20	3.29	0.19	0.17
8d	4.02	4.05	3.58	3.63	0.10	0.09
8e	0.00	0.00	0.00	0.00	42	43

8b. The molecule then goes through a boat form into a more stable twist form, **8c**, at the midpoint of the path. From there, the molecule proceeds further through a boat transition state, a twist minimum, **8d**, and a half-chair/sofa transition state before it ends up in the equatorial form, **8e**.

The gas-phase electronic energy of activation between minima **8a** and **8b** is calculated to be 4.86 kcal mol^{-1} (relative to **8e**), in moderately good agreement with the solvent phase 3.48(15) kcal mol^{-1} enthalpy of activation derived from the ^{19}F DNMR measurement. When the isodensity polarizable continuum model (IPCM) electronic energies of the minima (see later) are compared with the IPCM-calculated electronic energy of the gas-phase transition state, the agreement with the experimental values improves as the energy of activation decreases to 4.34 and 4.26 kcal mol^{-1} in chloroform and dichloromethane, respectively.

The gas-phase 0 K energies and 298 K free energies of the minima **8a−e** have also been calculated with the CBS-QB3[41,42] and G3B3[43] composite methods. The results are summarized in Table 4 together with the partial abundances of each conformer based on the 298 K free energies and the Boltzmann distribution. CBS-QB3 and G3B3 0 K energies are also plotted in Figure 7.

^{19}F NMR Shieldings. The absolute shielding constants of the fluorine nuclei were calculated with the gauge-independent atomic orbital (GIAO)[44] method with several methods and basis sets at the optimized 6-311+G(d,p) geometries (Table 5). The

(41) Montgomery, J. A., Jr.; Frisch, M. J.; Ochterski, J. W.; Peterson, G. A. *J. Chem. Phys.* **1999**, *110*, 2822.
(42) Montgomery, J. A., Jr.; Frisch, M. J.; Ochterski, J. W.; Peterson, G. A. *J. Chem. Phys.* **2000**, *112*, 6532.
(43) Baboul, A. G.; Curtiss, L. A.; Redfern, P. C.; Raghavachari, K. *J. Chem. Phys.* **1999**, *110*, 7650.
(44) Cheeseman, J. R.; Trucks, G. W.; Keith, T. A.; Frisch, M. J. *J. Chem. Phys.* **1996**, *104*, 5497.

Table 5. Calculated ^{19}F NMR Shielding Constants in 8a and 8e

	absolute shielding constant (ppm)		
method and basis set	**8a**	**8e**	difference (ppm)
MP2/6-311++G(2df,2pd)	398.5	388.6	9.9
B3LYP/6-311++G(2df,2pd)	376.6	367.0	9.7
PCM in $CHCl_3$[a]	380.8	371.5	9.3
B3LYP/aug-cc-pVTZ	381.9	371.8	10.1

[a] F shielding constant calculated within the PCM approach in chloroform at the gas-phase geometry and the B3LYP/6-311++G (2df,2pd) level.

Table 6. Solvation Effects[a]

	method							
			PCM(B3LYP)[b]		IPCM[c]		G3B3-corrected[d]	
	G3B3	B3LYP/ 6-311G(d)	$CHCl_3$	CH_2Cl_2	$CHCl_3$	CH_2Cl_2	$CHCl_3$	CH_2Cl_2
$\Delta E_{0\,K}$	−0.16	−0.26	−0.33	−0.36	−0.59	−0.50	−0.52	−0.43
$\Delta G_{112\,K}$			−0.35	−0.38	−0.61	−0.52	−0.54	−0.45

[a] Stabilization of the axial versus equatorial conformer in solution. $\Delta E_{0\,K}$ and $\Delta G_{112\,K}$ values are in kcal mol^{-1}. [b] Geometry optimization and ZPE correction based on analytical PCM force constants. [c] ZPEs and thermal contributions to the energy are taken from the corresponding PCM calculations. [d] The G3B3-corrected energies are based on 0 K G3B3 energies, ZPEs and thermal contributions are from the PCM calculations, and the solvent effect on the electronic energy is calculated with the IPCM approach.

magnitude of the relative shieldings is in excellent agreement with the experiment, and their sign confirms the expected assignment in which the fluorine nuclei are more shielded in the axial position than in the equatorial one. Solvation effects are insignificant because the absolute shieldings shift more if the 6-311++G(2df,2pd) basis set is exchanged for aug-cc-pVTZ than if the calculation is carried out in chloroform in the PCM framework.

Computational Studies in Solution. GED, ^{19}F DNMR, and Raman measurements confirmed that the axial conformer is more stable in both the gas phase at room temperature and the solvent phase at low temperatures. This is in contrast with **7**, which is stabilized in a freon solution, so that the equatorial conformer becomes dominant.[1] The PCM(B3LYP/6-311G(d))[45] and IPCM(B3LYP/6-311G(d))[46] approaches together with gas-phase B3LYP/6-311G(d) calculations were shown to reproduce the solvent effects accurately for **7**; therefore, we followed the same approach for **8**: the PCM method was used to study the geometry relaxation and the changes in the zero-point energy (ZPE) correction. Single-point IPCM energies were then calculated at the relaxed geometries. Dichloromethane and chloroform were used as solvents because these are parametrized in the PCM model and are believed to resemble the actual solvent mixture used in the ^{19}F NMR experiment. More precisely, CH_2Cl_2 is believed to represent an upper limit and $CHCl_3$ a lower limit of the solvation effects in the freon mixture.[1]

Both solvation methods predict a preference for the axial conformer in the polar solvents, which is in agreement with the experiments. To calculate the stabilization of the axial conformer in solution, the 0 K B3LYP solvation energies and the thermal contributions to free energy were added to the 0 K G3B3 energies. The results in Table 6 show a moderate stabilization effect on the order of 0.5 kcal mol^{-1}, which is, nevertheless, an overestimate of the ^{19}F DNMR experimental value (Table 3).

Conclusions

The conformational properties of **6** and **7** have previously been reported and compared with their cyclohexane analogues.[1,18] Substituted silacyclohexanes have lower energy barriers to conformational change and lower *A* values than the corresponding substituted cyclohexanes, but the trends and the lack of an overall equatorial preference in silacyclohexanes are in contrast to the behavior observed in cyclohexane derivatives. In the present work, **8** has been investigated by a number of experimental and computational structural chemistry techniques as a contribution to this field of study. In the gas phase, the findings of GED result in a negative *A* value (−0.31 kcal mol^{-1}), suggesting that the axial conformer, **8a**, is more stable. Likewise, two condensed-phase methods (Raman spectroscopy and NMR) also indicate that the axial conformer is favored in the neat liquid and in solutions in polar and apolar solvents as well. The negative *A* values are at variance with analogous results for the fluorinated cyclohexane derivative, for which a positive *A* value of 0.3 kcal mol^{-1} was found.[9] In silacyclohexanes, the electronegative fluoro and trifluoromethyl substituents both prefer the axial position in the gas phase, irrespective of their steric need, but the low-temperature stabilization of the equatorial conformer in a freon solution has only been observed in **7**,[1] and is absent in **8**. Both the observed axial preference in the gas phase and the unchanged axial preference observed in low-temperature DNMR have been successfully reproduced by computational chemistry methods, even though the low-temperature stabilization of the axial isomer, **8a**, in the solvent phase has been overestimated by the calculations.

A qualitative explanation for the missing equatorial stabilization in fluorosilacyclohexane with respect to **7** could be that the dipole moment of fluorosilacyclohexane is only 60–70% of that of trifluoromethylsilacyclohexane (RHF/GTlarge and B3LYP/6-31G(d) ratios, respectively, valid for both the axial and equatorial conformers), so the dipole–dipole interaction with the solvent molecules may be less strong in fluorosilacyclohexane.

Experimental Section

Materials. Compound **8** was prepared according to a general procedure described by Schott et al.[47] Chlorosilacyclohexane was prepared as described by West.[48]

1-Fluoro-1-silacyclohexane (8). HF (40%; 8 g, 160 mmol) was slowly added to 1-chloro-1-silacyclohexane (21.5 g, 160 mmol) at −30 °C. The reaction mixture was allowed to stand in the cooling bath and warm up slowly to room temperature. Afterward, it was transferred to a separation funnel, the aqueous phase was discarded, and the organic layer was dried over $MgSO_4$. The desired product was collected by distillation under reduced pressure (54 °C, 180 Torr) as a colorless liquid, analytically pure by NMR spectroscopy. Yield: 5.56 g (47 mmol, 29%). ^{1}H NMR (400 MHz, $CDCl_3$): δ 0.77–0.83 (m, 2H, $CH_{2(ax/eq)}$), 0.87–0.97 (m, 2H, $CH_{2(ax/eq)}$), 1.37–1.54 (m, 2H, CH_2), 1.67–1.84 (m, 4H, CH_2), 4.81 (d, $^2J_{H-F}$ = 54 Hz, 1H, SiH). ^{13}C{^{1}H} NMR (101 MHz, $CDCl_3$): δ 13.2 (d, $^2J_{F-C}$ = 11.1 Hz), 23.2 (d, $^3J_{F-C}$ = 1.0 Hz), 29.2. ^{19}F NMR (376 MHz, $CDCl_3$): δ −180.8 (dtm, $^2J_{H-F}$ = 54 Hz, $^3J_{H-F}$ = 11.1 Hz).

(45) Barone, V.; Cossi, M.; Tomasi, J. *J. Comput. Chem.* **1998**, *19*, 404.
(46) Foresman, J. B.; Keith, T. A.; Wiberg, K. B.; Snoonian, J.; Frisch, M. J. *J. Phys. Chem.* **1996**, *100*, 16098.
(47) Schott, V. G.; Schneider, P.; Kelling, H. *Z. Anorg. Allg. Chem.* **1973**, *398*, 293.
(48) West, R. *J. Am. Chem. Soc.* **1954**, *76*, 6012.

^{29}Si NMR (79 MHz, $CDCl_3$): δ 13.9 (d, $^2J_{Si-F}$ = 290 Hz). MS (EI, 70 eV): *m*/*z* (%) 118 (20) [M^+], 99 (100) [$M^+ - F$].

GED Experiment. Electron diffraction intensities were recorded with a Gasdiffraktograph KD-G2[49] at 25 and 50 cm nozzle-to-plate distances and with an accelerating voltage of about 60 kV. The electron wavelength was derived from ZnO powder diffraction patterns. The sample was kept at −10 °C during the experiment, and the inlet system and nozzle were at room temperature. The photographic plates (Kodak Electron Image Plates, 18 × 13 cm) were analyzed with an Agfa Duoscan HiD scanner, and total scattering intensity curves were obtained using the program *SCAN3*.[50] Averaged experimental molecular intensities in the range s = 2–30 Å^{-1} in steps of Δs = 0.2 Å^{-1} ($s = (4\pi/\lambda) \sin\theta/2$, where λ is the electron wavelength and θ is the scattering angle) are available as Supporting Information.

Low-Temperature NMR Experiment. A solvent mixture of CD_2Cl_2, $CHFCl_2$, and CHF_2Cl in a ratio of 1:1:3 was used for the low-temperature ^{19}F NMR measurements. The temperature of the probe was calibrated by means of a type K (chromel/alumel) thermocouple inserted into a dummy tube the day before and the day after the NMR experiment. The readings are estimated to be accurate within 2 K. The NMR spectra were loaded into the data-handling program IGOR (WaveMetrics) for analysis, manipulations, and graphic display. Line-shape simulations of the NMR spectra were performed with a PC version of the DNMR program (QCPE program no. 633; Indiana University, Bloomington, IN), kindly offered by Professor L. Lunazzi.[51]

Low-Temperature Raman Experiment. Raman spectra were recorded with a Jobin Yvon T64000 spectrometer equipped with a triple monochromator and a CCD camera. The samples were filled into 1 mm capillary glass tubes and irradiated by the green 532 nm line of a frequency-doubled Nd:YAG laser (Coherent, DPSS model 532-20, 20 mW). The spectra of the pure compound and that in pentane and dichloromethane solutions were recorded. A continuous-flow cryostat (Oxford Instruments OptistatCF) using liquid nitrogen for cooling was employed for the low-temperature measurements.

(49) Oberhammer, H. *Molecular Structure by Diffraction Methods*; The Chemical Society: London, 1976; Vol. 4, p 24.
(50) Atavin, E. G.; Vilkov, L. V. *Instrum. Exp. Tech.* **2002**, *45*, 745.
(51) Courtesy of Lunazzi, L., University of Bologna, Bologna, Italy.

Acknowledgment. We acknowledge the computational facilities made available by Prof. Paul Mezey, Director, Scientific Modeling and Simulation Laboratory, Memorial University of Newfoundland. The Austrian "Fonds zur Förderung der wissenschaftlichen Forschung" is also gratefully acknowledged for financial support (Project P-17435). A.V.B., A.A.B., and H.O. thank the Deutsche Forschungsgemeinschaft for financial support of the German−Russian Cooperation Project GZ:436/RUS 113/69/0-6. Financial support from the "University of Iceland Research Fund" is gratefully acknowledged.

Supporting Information Available: Tables containing interatomic distances, vibrational amplitudes, Cartesian coordinates, and the radial distribution curve for the GED experiment, selected Raman spectra, peak positions, and van't Hoff plots for pure **8** and that in pentane and dichloromethane solutions, calculated optimized geometries and energies of the minima and the transition states, and the full author list of ref 40. This material is available free of charge via the Internet at http://pubs.acs.org.

OM7008414